Korean J. Chem. Eng., **26**(5), 1341-1352 (2009)
DOI: 10.2478/s11814-009-0197-4

Surface modification and adsorption of eucalyptus wood-based activated carbons: Effects of oxidation treatment, carbon porous structure and activation method

Chaiyot Tangsathitkulchai*,†, Yuvarat Ngernyen*, and Malee Tangsathitkulchai**

*School of Chemical Engineering, Institute of Engineering, Suranaree University of Technology, Nakhon Ratchasima 30000, Thailand
**School of Chemistry, Institute of Science, Suranaree University of Technology, Nakhon Ratchasima 30000, Thailand
(*Received 23 November 2008 • accepted 6 February 2009*)

Abstract−The incorporation of oxygen functional groups onto the surface of eucalyptus activated carbon and its surface chemistry were investigated as a function of oxidation conditions, carbon porous properties and carbon preparation method. Under all treatment conditions of increasing time, temperature and oxidant concentration, liquid oxidation with HNO_3, H_2O_2 and $(NH_4)_2S_2O_8$ and air oxidation led to the increase of acidic group concentration, with carboxylic acid showing the largest percentage increase and air oxidation at the maximum allowable temperature of 350 °C produced the maximum content of both carboxylic acid and total acidic group. Nitric acid oxidation of chemically activated carbon produced higher total acidic content but a lower amount of carboxylic acid compared to the oxidized carbon from physical activation. The increased contents of acidic groups on oxidized carbons greatly enhanced the adsorption capacity of water vapor and heavy metal ions.

Key words: Activated Carbon, Adsorption, Oxygen Functional Groups, Surface Modification, Carbon Porous Structure

INTRODUCTION

The adsorption capacity of an activated carbon depends both on the physical porous structure as well as the chemical properties of the carbon surface [1]. The surface chemistry of activated carbons is primarily determined by the acidic and basic properties of their surfaces [2]. The acidic property of the carbon is associated with oxygen functionalities such as carboxylic acid, lactones and phenols. The basic properties, however, are ascribed both to Brönsted basic functional groups (e.g., pyrones, carbonyls, chromenes, quinones and ethers) and the oxygen-free Lewis basic sites which are associated with π electron density within the carbon basal planes [2, 3-8]. The less polar or non-polar adsorbate is generally adsorbed on the non-polar graphene layers by dispersive forces that depend on the nature of carbon porous structure. However, for the adsorption of a polar adsorbate or an ionic species, the adsorption takes place preferentially on the hydrophilic site of oxygen functional groups by electrostatic interaction [9]. Fixation of more oxygen functional groups on the surface of activated carbon would impart more hydrophilic character which promotes the adsorption of polar or ionic adsorbates.

Additional oxygen functional groups can be introduced by oxidation with such oxidants as air, ozone, hydrogen peroxide and nitric acid, resulting in the formation of higher content of acidic groups and a lesser content of basic sites [7,9-13]. While oxidation in the gas or liquid phase can be used to increase the concentration of surface functional groups, heating under an inert atmosphere may be used to selectively remove some of these functional groups [14,15]. Several investigators have studied the role of surface chemistry, oxygen content and porous properties of activated carbon on its adsorption of metal ions (Cd^{2+}, Cu^{2+}, Hg^{2+}, Pb^{2+} and Zn^{2+}) [6,9,14,16-19], aromatic species, (phenol and nitrobenzene) [20,21], polar adsorbates (water vapor) [11,22-24], SO_2 and methanol [25] and nonpolar adsorbates (N_2 and CO_2) [25].

Although many reports deal with the oxidation of activated carbons and their adsorption performance, different conclusions often exist. This is because the degree of oxidation of activated carbon and type of surface groups created during the oxidation process depend on a number of factors such as the type of oxidizing agent, oxidation conditions and type of precursors [6,7,26-28]. The adsorption phenomenon is also complicated, especially for the adsorption in liquid phase where the adsorption capacity of an activated carbon depends on such factors as the nature of adsorbent (surface area, pore size distribution, functional groups) and adsorbate (polarity, size, pKa, functional groups) as well as solution conditions (pH, temperature). Due to the many factors that are involved in the adsorption process, the result of adsorbate-adsorbent interaction is often different for each system, and this necessitates its own investigation to arrive at the most precise adsorption mechanisms [1,9,17,19,20].

The present study explored in detail the changes in surface chemistry and porous properties of a series of chemically activated carbon from eucalyptus wood that was oxidized by four oxidizing agents and with different degrees of oxidation. Eucalyptus wood was used as a starting precursor, for activated carbons with varied porous properties from low to relatively high surface area can be conveniently produced from this type of material [29-31]. In addition, activated carbons prepared by physical activation having different surface area and porosity were oxidized to investigate the influence of porous structure on the quantity and distribution of the introduced surface

†To whom correspondence should be addressed.
E-mail: chaiyot@sut.ac.th

functional groups. Selective removal of the surface functional groups by thermal treatment under an inert atmosphere was also investigated. The results from surface modification of the activated carbons prepared from different activation methods and those having different porous structures would lead to a better understanding of the effect of surface treatment with respect to the properties of these carbons. The final part of this work involved the adsorption of water vapor and metal ions on activated carbons before and after oxidation and after thermal treatment. Here, the nature of interaction between the activated carbon surface chemistry and adsorptive molecules could be assessed.

MATERIALS AND METHODS

1. Preparation of Activated Carbons

Eucalyptus wood-based activated carbons prepared by both chemical and physical activation were used in the study of surface modification and chemistry. Activated carbon prepared by chemical activation with H_3PO_4 was employed to study the effect of oxidizing agents and treatment conditions on the incorporation of surface functional groups. Activated carbons prepared by physical activation with CO_2 were selected to study the effects of porous structure and heat treatment on the amount and distribution of surface functional groups.

Eucalyptus wood (*Eucalyptus camaldulensis Dehn*.) in the form of shaving was milled and sieved to obtain a size fraction of 20×30 mesh (average size 0.714 mm). For the preparation of activated carbon by chemical activation (sample C), the pre-dried sample was impregnated for 1 h with 50 wt% concentration of H_3PO_4 by using a 0.5 : 1 chemical weight ratio of H_3PO_4 and wood. The mixture was carbonized in a tube furnace (Carbolite, UK) at 400 °C for 1 h under a constant supply of N_2. After carbonization, the resulting carbon was washed and dried. For preparing the activated carbon by physical activation, the wood sample was first carbonized in a tube furnace at 400 °C for 1 h in the atmosphere of flowing N_2 and further activated with CO_2 for 1 h at 600, 800 and 900 °C (samples PA, PB and PC).

2. Oxidation of Activated Carbons

Three oxidizing agents were used for the liquid phase oxidation, including H_2O_2, $(NH_4)_2S_2O_8$ and HNO_3. After oxidation the carbon products were thoroughly washed and dried. Details of oxidation conditions and methods are shown in Table 1. For the gas phase oxidation, the activated carbon sample was heated in a packed bed reactor (2.5 cm I.D. by 10 cm long) inserted in the tube furnace from room temperature to the set temperature under the constant flow of N_2. When the final temperature was attained, N_2 flow was switched to air at the rate 100 cm^3/min for the required treatment time. Then, the furnace was cooled to room temperature under the flow of N_2 and the oxidized product was kept for subsequent characterization.

3. Heat Treatment of Oxidized Carbon

The activated carbon prepared by physical activation at the activation temperature of 800 °C was oxidized with 1 M HNO_3 for

Table 1. Treatment methods and conditions

Treatment method	Sample codes	Treatment conditions
Original carbon (chemical activation)	C	H_3PO_4 : wood (0.5 : 1), 400 °C, 1 h
H_2O_2 oxidation	CH-24	35 wt% H_2O_2, 25 °C, 24 h
	CH-48	35 wt% H_2O_2, 25 °C, 48 h
$(NH_4)_2S_2O_8$ oxidation	CM-24	sat. sol. $(NH_4)_2S_2O_8$ in 1 M H_2SO_4, 25 °C, 24 h
	CM-48	sat. sol. $(NH_4)_2S_2O_8$ in 1 M H_2SO_4, 25 °C, 48 h
HNO_3 oxidation (reflux)	CN1-12	1 M HNO_3, 80-90 °C, 12 h
	CN1-24	1 M HNO_3, 80-90 °C, 24 h
	CN1-48	1 M HNO_3, 80-90 °C, 48 h
	CN5-24	5 M HNO_3, 80-90 °C, 24 h
	CN10-24	10 M HNO_3, 80-90 °C, 24 h
Air oxidation	CA1-12	air, 250 °C, 12 h
	CA1-24	air, 250 °C, 24 h
	CA1-48	air, 250 °C, 48 h
	CA2-24	air, 350 °C, 24 h
Original carbon (*physical activation*)	PA	CO_2, 600 °C, 1 h
	PB	CO_2, 800 °C, 1 h
	PC	CO_2, 900 °C, 1 h
HNO_3 oxidation (reflux)	PA1	1 M HNO_3, 80-90 °C, 24 h
	PA5	5 M HNO_3, 80-90 °C, 24 h
	PB1	1 M HNO_3, 80-90 °C, 24 h
	PB5	5 M HNO_3, 80-90 °C, 24 h
	PB10	10 M HNO_3, 80-90 °C, 24 h
	PC1	1 M HNO_3, 80-90 °C, 24 h
	PC5	5 M HNO_3, 80-90 °C, 24 h
	PC10	10 M HNO_3, 80-90 °C, 24 h
Heat-treatment	PB1-HT1	N_2, 600 °C, 12 h
	PB1-HT2	N_2, 800 °C, 12 h

24 h (sample PB1) and heated in the packed-bed reactor at the required temperature under the N_2 atmosphere for 12 h. The heat treatment conditions and sample codes are also shown in Table 1.

4. Characterization of Carbon Properties

Porous properties of the activated carbons were determined from N_2 adsorption isotherm data at −196 °C acquired by an automated adsorption apparatus (ASAP 2010, Micromeritics). From the isotherm data, the specific surface area, S_{BET}, was estimated by applying the Brunauer-Emmett-Teller (BET) equation [32]. The micropore volume, V_{mic}, was calculated by applying the Dubinin-Radushkevich (DR) equation [32]. The total pore volume, V_T, was found from the amount of N_2 gas adsorbed at the relative pressure of 0.99 and converting it to the corresponding volume in liquid state.

Boehm titration [33,34] is the selective neutralization method used to evaluate the carbon surface acidity and basicity. One gram of activated carbon was mixed with 100 cm^3 of 0.1 M solutions of HCl, NaOH and $NaHCO_3$ and 0.05 M Na_2CO_3. Each vial was shaken for 24 h and the suspension filtered. The filtrate solutions of NaOH, Na_2CO_3 and $NaHCO_3$ were titrated with 0.1 M HCl, while the filtrate solution of HCl was titrated with 0.1 M NaOH. The titrant volumes of the various bases and acids were used to determine the amounts of acidic groups (carboxylic acid, phenolic and lactonic) and basic sites on the activated carbon surface.

An FTIR spectrometer (FTS175C, BIO-RAD) was used to measure the infrared spectrum of the activated carbons for identifying their chemical functionalities. The activated carbon was mixed with KBr powder and the pellet was formed by compressing at 10 tons for 2 min in a hydraulic press. Before measurement, the instrument was run to collect the background, which was automatically subtracted from the sample spectrum.

The XPS (X-ray photoelectron spectroscopy) spectra were collected by using a Mg Kα X-ray source (1253.6 eV). The activated carbon sample was placed in the pretreatment chamber and degassed at 10^{-6} mbar. Then, it was transferred to the ion-pumped analysis chamber, in which residual pressure is kept below 4×10^{-9} mbar during data acquisition. The C_{1s} peak of the sample was analyzed in the binding energy range of 275-295 eV. The O_{1s} peak was analyzed in the binding energy range of 525-545 eV. The accuracy of the binding energy is ±0.1 eV.

Elemental analysis of C, H, N and O contents was determined by using a CHN/O analyzer (CHN/O-932, LECO).

The pH_{pzc} was determined by adjusting the pH of 0.01 M NaCl (50 cm^3) to values between 1 to 10, obtained by adding either 0.1 M HCl or NaOH. About 0.15 g of activated carbon was added into each respective solution at room temperature and then shaken for 48 h. The final pH was measured and plotted against the initial pH. The pH at which the plotted curve intersected the 45° line (pH_{final}= $pH_{initial}$) was taken as the pH_{pzc} of the activated carbon surface.

5. Adsorption Studies

5-1. Water Vapor Adsorption

Adsorption of water on the activated carbon sample was by an Intelligent Gravimetric Analyzer (IGA 002, Hiden Analytical, UK). This instrument is fully computer controlled and measures the amount adsorbed via a microbalance. Prior to the adsorption measurement, the carbon sample was out-gassed at 250 °C and a vacuum pressure of 75 mmHg for about 5 h. Mass uptake of water vapor was measured as a function of time until the equilibrium was reached for each increasing step of pressure up to the value close to the saturation vapor pressure, where bulk condensation of water from gas phase occurs.

5-2. Heavy Metal Adsorption

Batch adsorption tests of metal cations in aqueous solutions were performed as follows. Each stock solution of 10 mM of Pb^{2+}, Cu^{2+} and Ca^{2+} was prepared from $Pb(NO_3)_2$, $Cu(NO_3)_2.3H_2O$ and $Ca(NO_3)_2\cdot4H_2O$, respectively. Different concentrations of metal ions in solutions were prepared by diluting the initial stock solution and 0.1 g of carbon sample was added into a volume of 50 cm^3 of each solution. The mixture was shaken in a water-bath shaker kept at 30 °C for 72 h to attain adsorption equilibrium without adjusting the solution pH. The pH values of the solution before and after adsorption were also noted. The concentrations of metal ions in solution were measured by an Inductive Coupled Plasma (ICP) atomic emission spectrometer (Model 701, Unicam).

RESULTS AND DISCUSSION

1. Properties of Original Activated Carbons

Fig. 1 shows the porous properties and chemical surface contents of original activated carbons prepared by chemical activation (sample C) and physical activation (samples PA, PB and PC). As seen, the surface area and pore volume of the original carbons show the following order, PC>C>PB>PA, and the porous structures of all original carbons exhibit mainly microporosity (>82%). It was found that adsorption isotherms of these carbons displayed Type I isotherm according to IUPAC classification system [35], thus further confirming the typical microporous nature of these activated carbons.

As to the acidic surface groups, Fig. 1 indicates that the original carbon prepared by chemical activation had much lower amount of total acidic groups compared to the physically activated carbons. It is probable that the physically activated carbons could contain greater surface defects due to bond disruption caused by a much

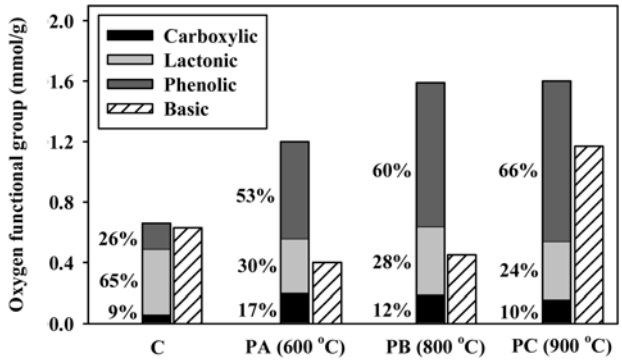

	C	PA (600 °C)	PB (800 °C)	PC (900 °C)
Acidic group (mmol/m^2)	5.50×10^{-4}	2.61×10^{-3}	2.44×10^{-3}	1.07×10^{-3}
S_{BET} (m^2/g)	1200	460	651	1491
V_{mic} (cm^3/g)	0.55 (95%)	0.21 (91%)	0.29 (88%)	0.66 (82%)
V_T (cm^3/g)	0.58	0.23	0.33	0.80

Fig. 1. Chemical surface content and porous properties of the original activated carbons prepared by chemical (C) and physical activations (PA, PB and PC).

higher activation temperature (600-900 °C versus 400 °C), thus promoting the creation of functional groups by CO_2 during the activation treatment.

Fig. 1 also presents the concentration of acidic surface groups in terms of surface density in mmol/m^2 of total surface area. It is clear that sample C gave the lowest acidic group density despite its relatively high surface area. For physically activated carbons, samples PA and PB showed similar acidic surface group densities, indicating that at these two activation temperatures the amount of acidic groups introduced during activation is proportional to the developed surface area. This is expected since the fixation of acidic surface groups and pore development occur in parallel during the course of gasification reaction with CO_2 [1]. However, a too high activation temperature of 900 °C would cause the detachment of some acidic groups due to their thermal instability, hence lowering the acidic group density of sample PC.

Apart from the difference in total acid quantity, the differences in the amount and distribution of acid types of oxygen functional groups are also discernible between the original activated carbons prepared from chemical and physical activation. As noticed from Fig. 1, sample C contained the highest amount of lactonic group (65%) followed by phenolic group (26%) and carboxylic acid (9%), whereas samples PA, PB and PC gave the amounts of acidic group in the following order: phenolic>lactonic>carboxylic. For original carbons obtained from physical activation, the increasing of activation temperature also affected the quantity and percentage distributions of each acidic surface group. There is a tendency that the percentage distribution of carboxylic acid and lactonic groups was decreased while that of phenolic group was increased with increasing activation temperature from 600 to 900 °C. The amount of basic sites was found to increase with increasing in the activation temperature, with a marked increase being observed at 900 °C. In comparison with the acidic groups, the higher proportional increasing of basic sites at the activation temperature of 900 °C should result from the effect of their higher thermal stability at this high activation temperature [21].

Table 2. Porous characteristics of the original, oxidized and heat treated activated carbons

Sample	S_{BET} (m^2/g)	V_{mic} (cm^3/g)	V_T (cm^3/g)
Effect of oxidizing agents			
C (original carbon)	1200	0.55 (95%)	0.58
CH-24	689	0.34	0.35
CM-24	738	0.34	0.36
CN1-12	590	0.28	0.31
CN1-24	523	0.26	0.27
CN5-24	NM[a]	NM	NM
CA1-12	794	0.37	0.39
CA1-24	626	0.29	0.31
CA1-48	585	0.27	0.28
CA2-24	NM	NM	NM
Effect of porous structure			
PA (original carbon)	460	0.21 (91%)	0.23
PA1	405	0.20	0.23
PA5	NM	NM	NM
PB (original carbon)	651	0.29 (88%)	0.33
PB1	604	0.26	0.32
PB5	NM	NM	NM
PB10	NM	NM	NM
PC (original carbon)	1491	0.66 (82%)	0.80
PC1	1161	0.50	0.68
PC5	NM	NM	NM
PC10	NM	NM	NM
Effect of heat treatment			
PB1 (oxidized carbon)	604	0.26	0.32
PB1-HT1	647	0.29	0.34
PB1-HT2	774	0.35	0.40

[a]NM=not measurable

2. Effect of Surface Treatments on the Porous Properties of Oxidized Carbons

Porous properties data are shown in Table 2 for the original activated carbons, oxidized carbons and heat-treated oxidized carbons. The incorporation of oxygen functional groups by oxidation treatments of all carbon samples caused a decrease in their porous properties. The degree of this decrease intensified with increasing in the strength and concentration of oxidants as well as the oxidation time. It is also noted that the porous properties could not be measured for those oxidized samples having high oxygen surface group creation, including samples CA2-24, PA5, PB5, PB10, PC5 and PC10. When examining the typical nitrogen adsorption isotherms of carbon samples from which the porous properties were determined, it was found that the amounts of nitrogen adsorbed also decreased for all the oxidized samples. Thus, it is reasonable to infer that the lowering in the surface area and pore volume of oxidized carbons is the result of an inaccessibility of the probe nitrogen molecules into the internal adsorption sites caused by the presence of increased surface groups at the pore entrance of the graphitic basal planes and possibly by the collapse of some thin pore walls due to the strong action of oxidizing agents [11,19,36]. As expected, the thermal treatment of oxidized carbon (sample PB1) at high temperatures (600 and 800 °C) in an inert atmosphere would cause the detachment of some surface functional groups, giving rise to the restoration of its porous properties. Too high of the thermal treatment temperature (800 °C), however, could even create higher porosity and surface area than those of the original carbon, possibly by the loss of carbon mass through the forming of liberated CO and CO_2.

3. Effect of Surface Treatments on Surface Chemistry of Oxidized Carbons

Boehm titration results of the original and oxidized activated carbons are shown in Fig. 2. All oxidation treatments produced considerable amount of acidic surface groups in the carbons. In all cases, increasing the degree of oxidation treatments (increasing temperature, time, strength and concentration of oxidizing agents) resulted in a corresponding increase in the number of total acidic surface groups. Conversely, the basic site content decreased after oxidation except with the nitric acid treatment where the opposite effect could be observed. With reference to acidic group content of the oxidized carbon, the following order was noted: lactonic>phenolic>carboxylic acid, for H_2O_2 and $(NH_4)_2S_2O_8$ oxidation; phenolic>lactonic>carboxylic acid, for HNO_3 oxidation; and carboxylic acid>lactonic>phenolic, for air oxidation. The percent increase of acidic types in all oxidized carbons as compared to the original activated carbon was

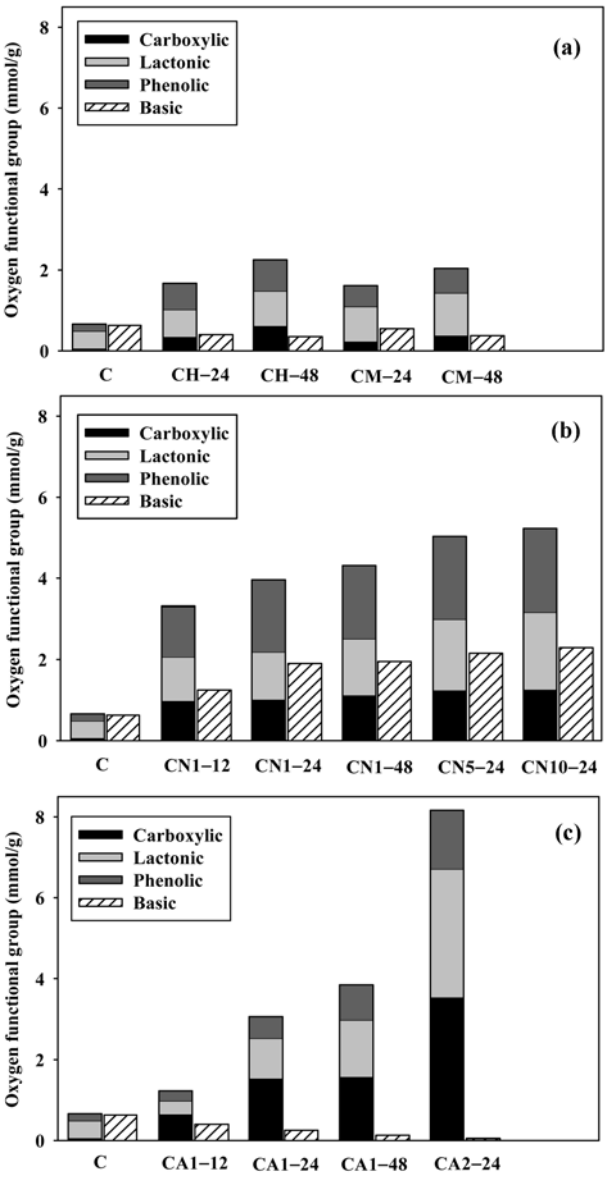

Fig. 2. Chemical surface content of the original activated carbon and activated carbons oxidized with H_2O_2 and $(NH_4)_2S_2O_8$ (a), HNO_3 (b), and air (c).

highest for the carboxylic acid, followed by phenolic and lactonic groups. For example, oxidizing the original carbon with air at 250 °C for 24 h (sample CA1-24) increased the content of carboxylic acid, phenolic and lactonic groups by 2450%, 212% and 132%, respectively. The carboxylic acid has relatively high ion-exchange capacity than other oxygen surface groups and as a result the large increase in carboxylic acid content is advantageous for efficient separation of positively charged adsorbates like metal cations in aqueous solution.

It is further noticed that liquid phase oxidation produced the least quantity of carboxylic acid as compared to weaker phenolic and lactonic groups, whereas air oxidation gave the largest creation of carboxylic acid. The relatively high carboxylic acid content from air oxidation could result from the disruption of the carboncarbon bond at the high oxidation temperature, leading to higher oxidation susceptibility to form dicarboxylic acid. This C-C bond cleavage is expected to occur more easily in the activated carbon prepared from wood which has much less conjugated ring structure in the carbon [10]. The overall effect would thus lead to the formation of more carboxylic acid, giving a maximum increase of its content by almost 60 times for air oxidation at 350 °C and 24 h (sample CA2-24) compared to the original sample C, whereas the maximum increase of this surface group was only 20 times for liquid-phase HNO_3 oxidation (sample CN10-24). However, the notably high content of carboxylic acid by air oxidation at 350 °C as determined by Boehm titration may include carboxylic anhydride since it is possible that during the oxidation treatment adjacent carboxylic groups could be dehydrated into carboxylic anhydride [12,37]. The carboxylic anhydride on the carbon surface can be hydrolyzed in aqueous solution rendering two carboxylic groups, which as well can be analyzed as carboxylic acid content by Boehm titration [38].

Similar study but with different results was reported by Goyal et al. [14] who found that oxidation of bituminous coal-based activated carbon with nitric acid produced higher acidic surface groups than with gaseous oxygen. In addition, by using steam activated carbon from apricot stone, Strelko et al. [27] reported that air oxidation gave a higher proportion of relatively weaker acid groups (lactonic and phenolic), whereas nitric acid oxidation yielded higher content of stronger carboxylic acid. Differences in the nature of raw material, oxidation conditions and method of characterization for surface chemistry probably gave rise to the inconsistency between these results and those obtained in the present work.

It was found that all oxidation treatments in this work produced less basic content than acidic content. However, when compared with the original carbon, the basic contents showed a small decrease with H_2O_2 and $(NH_4)_2S_2O_8$ treatments and a large decrease with air treatment, whereas an increase of basic content was observed for nitric acid oxidation (Fig. 2). In spite of the fact that some oxygen functionalities are able to act as basic sites, some authors [2-7,39] have reported that the basic sites can be oxygen-free Lewis type, which are associated with π electron density within the carbon basal planes. Thus, the variation of this Lewis basic site content can be influenced by the nature of electron donating or electron withdrawing of acidic groups situated at the edges of graphene layers. It is noted that carbons oxidized with nitric acid in this work contain the largest proportion of phenolic group, which is an electron donating group that can increase the π-electron density on the graphene planes. As a result, this would lead to an observed increase in the basic content of HNO_3 oxidized carbon. On the other hand, the reduction in the basic content of H_2O_2 and $(NH_4)_2S_2O_8$ and air treatments should be due to the presence of highest proportion of electron withdrawing groups (i.e., lactonic and carboxylic groups) in these oxidized carbons. Based on this reasoning, the results presented here tend to support the view that the main contribution to carbon surface basicity is not from the basic functional groups at the edges of carbon crystallites but possibly from oxygen-free Lewis basic sites within the graphene planes.

Typical FTIR results of the original and some oxidized activated carbons are shown in Fig. 3. Observation of the absorption bands shows that the differences in transmission between the original and oxidized activated carbons are mainly due to the formation of oxygen functional groups. The most characteristic changes with respect to the new band or the increasing intensity of the bands were ob-

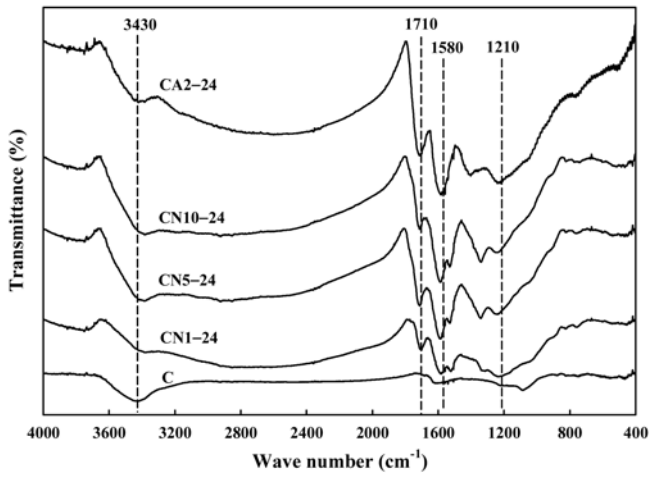

Fig. 3. FTIR spectra of the original and oxidized activated carbons.

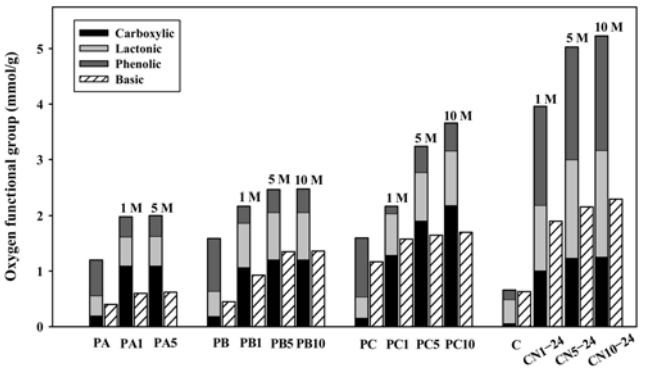

Fig. 4. Effect of activation method and HNO_3 concentration on chemical surface content of oxidized carbons.

served between four regions: around 3,430 cm^{-1}, 1,710 cm^{-1}, 1,580 cm^{-1} and 1,210 cm^{-1}. The new band at 1,710 cm^{-1} is ascribed to the stretching vibration of carboxyl groups on the edges of graphitic layer planes or to conjugated carbonyl groups (C=O in carboxylic acid and lactonic groups). The bands observed at 3,430 cm^{-1}, 1,580 cm^{-1} and 1,210 cm^{-1} are assigned to phenolic O-H stretching vibrations conjugated with C=O, C=O stretching vibrations, and O-H bending modes, respectively [19]. In those regions, the pronounced bands followed the order, CA2-24>CN10-24>CN5-24>CN1-24>C, and this order is also consistent with the results from Boehm titration.

The compositions of carbon and oxygen content at the external surface of the activated carbon particles can be obtained from analyzing the spectra of X-ray photoelectron spectroscopy (XPS). The O_{1s} and C_{1s} peaks are identified at the binding energy of about 533.2 and 284.6 eV, respectively. To calculate the percentage of surface atomic concentration, the peak areas of C_{1s} and O_{1s} were determined by applying the Gaussian equation and dividing by a sensitivity factor (0.205 for carbon and 0.63 for oxygen) [40]. Table 3 compares the surface atomic concentration of oxygen and carbon of the original and oxidized activated carbons. The order of oxygen content in the samples, which also supports the results from Boehm titration, is as follows: CN1-24>CH-24>C.

To further confirm the existence of increased oxygen functional groups on the activated carbon surfaces, elemental analyses were performed and the results are shown in Table 3. The order of oxygen content with reference to different oxidized carbons is in agreement with that of the amount of acidic surface groups from Boehm titration. Based on the results from XPS and the elemental analyses, it is noted that the functional group concentration at the external carbon surface and in the bulk solid is somewhat different after the oxidation treatment.

The values of pH_{pzc} are also illustrated in Table 3. As seen, all the oxidized carbons exhibited lower pH_{pzc} values than that of the original activated carbon. The lower values come from the negative charge surface of oxidized carbons in aqueous solution resulting from the dissociation of their acidic surface groups. The order of the pH_{pzc} was opposite to that of Boehm titration in that the higher content of acidic surface groups yielded the lower pH_{pzc} value.

4. Effect of Carbon Porous Structure on Chemical Surface Contents

To illustrate the effect of carbon porous structure on the variation in quantity and distribution of surface functional groups, three activated carbon samples with varying porous properties were prepared by physical activation with CO_2 at 600, 800 and 900 °C for 1 h (samples PA, PB and PC) and oxidized with nitric acid by boiling in a reflux condenser for 24 h. Fig. 4 shows the obtained results. It is observed that the content of total acidic groups and basic sites was increased after oxidation for each original carbon and the percent increase depended on both the available surface area of the original carbons and the concentration of HNO_3 used. Interestingly, for all oxidized carbons the general order of % increase and % distri-

Table 3. Elemental analysis, XPS analysis and pH_{pzc} of the original and oxidized activated carbons

Sample	C_{1s}[a] (%)	O_{1s}[a] (%)	C (wt%)	H (wt%)	O (wt%)	N (wt%)	pH_{pzc}
C	83.36	16.64	79.68	2.74	17.15	0.43	7.5
CH-24	71.14	28.86	74.10	3.18	22.37	0.35	6.6
CM-24	-	-	75.29	2.86	21.42	0.43	6.9
CN1-24	56.77	42.23	61.43	2.82	33.98	1.77	3.7
CN5-24	-	-	60.98	2.76	34.41	1.85	2.8
CN10-24	-	-	-	-	-	-	2.7
CA1-24	-	-	72.81	2.96	23.57	0.66	5.1
CA2-24	-	-	61.50	1.83	35.75	0.92	2.2

[a]From XPS analysis

bution of acidic groups was the same with carboxylic>lactonic> phenolic. The drop in phenolic content after oxidation may be due to the possible condensation of adjacent carboxylic acid and phenolic group to lactonic group [34,37]. Again, the increasing of nitric acid concentration tended to cause an increase in the chemical surface content of all oxidized carbons. In addition, increasing acid concentration appeared to have no influence on the relative proportion of each acidic group of the oxidized carbons. It is further noted that there exists a minimum nitric acid concentration that can produce a maximum content of total acidic surface group, and this optimum nitric acid concentration tends to increase proportionally with increasing surface area of the original carbons. Thus, in order to obtain fully oxidized surfaces for PA, PB and PC, the optimum HNO_3 concentration used would be 1 M, 5 M and around 10 M, respectively. Further analysis of these data reveals that for each original carbon, the ratio of maximum acidic content and its micropore surface area (400, 495 and 1,020 m^2/g for samples PA, PB and PC, respectively) appears to be relatively constant with the average value of 4.54×10^{-3} mmol/m^2. It is interesting that this number may be used for estimating the maximum creation of acidic surface groups for any physically activated carbon prepared from eucalyptus wood, requiring only its micropore area without the need to carry out the time-consuming HNO_3 oxidation and surface chemistry characterization.

The effect of preparation method of activated carbon on the introduced acidic surface groups can be observed from Fig. 4. Upon oxidation, the original carbon prepared by chemical activation and physical activation showed the differences in both the amount and distribution of the acidic surface groups. The original carbon prepared from chemical activation (sample C) contained lower content of total acidic groups than all carbons prepared by physical activation. However, after HNO_3 oxidation under the same treatment conditions, sample C created much higher total acidic groups than samples PA, PB and PC, although sample C contained lower surface area than sample PC. The physically activated carbon contains large condensed aromatic basal planes resulting from the high activation temperature, whereas the chemically activated carbon prepared at the lower temperature, has much fewer conjugated ring structures [10]. This makes the chemically activated carbon more susceptible to oxidation than the physically activated carbon, hence producing a larger number of acidic surface groups. It is noted that the amount of each acidic group present in the oxidized carbon of physically activated carbon followed the order: carboxylic>lactonic>phenolic, while the reverse order was true for the oxidized carbons originally prepared by chemical activation. The higher carboxylic acid content than the other two acidic groups of physically activated carbon could be a consequence of surface characteristics of these carbons which may contain more bond disruption resulting from high activation temperatures. Thus, it is logical to infer from this finding that under the same oxidation conditions, the type and amount of acidic surface groups introduced will depend not only on the available surface area of the original carbon but also on the activation method (chemical or physical) used.

Further examining the acidic contents of all oxidized carbons in this work showed that, within the limit of data variability, the distribution of acidic group content can be separated into two distinct groups depending on the level of temperature treatment. The first

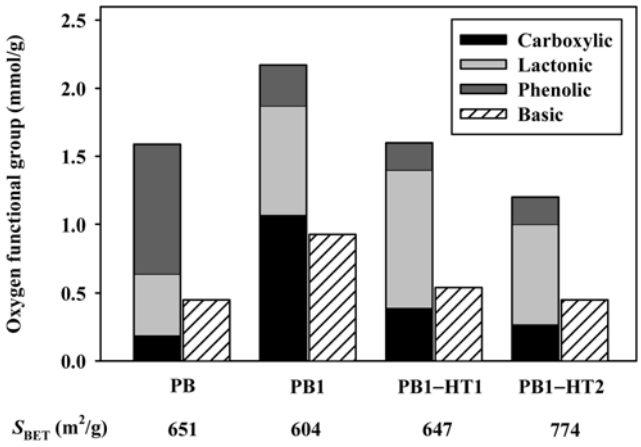

Fig. 5. Chemical surface content and the porous properties of the original, oxidized, and heat treated activated carbons.

group, which involves using activated carbons prepared at high activation temperatures (samples PA1, PB1, PC1) or oxidizing the carbon at relatively high temperatures (samples CA112, CA1-24, CA1-48, CA2-24), gives the highest content of carboxylic acid. The second group is related to the application of low oxidizing temperature (oxidation with H_2O_2, $(NH_4)_2S_2O_8$ and HNO_3) from which a maximum creation of lactonic group is achieved. Therefore, activation temperature and/or oxidizing temperature may be used to manipulate the creation and distribution of various acidic surface groups in the oxidized carbon obtained from eucalyptus wood, at least under the carbon preparation and oxidation conditions used in the present study.

The effect of thermal treatment on the variation of oxygen functional groups was studied by heating the oxidized carbon (PB1) at 600 °C and 800 °C for 12 h under the inert atmosphere of N_2 (sample PB1-HT1 and PB1-HT2) (see Fig. 5). After thermal treatment, both total acidic and basic sites were found to decrease, with higher treatment temperature giving higher percent reduction. This reduction is largest for the carboxylic acid group, which is the least stable form of the acidic types [12,37], whereas the amounts of lactonic and phenolic groups showed much less variation, indicating that they are more stable toward heat treatment. The heat treatment at 600 °C reduced the total acidic group content and increased the surface area to approximately those of the original carbon. However, the order of acidic group distribution appeared to be different between the two carbons. Thermal treatment at the higher temperature of 800 °C could further remove the total acidic group content by almost 50% of the oxidized carbon, with the resulting order of acidic group distribution being the same as that of treatment at 600 °C, i.e., lactonic >phenolic>carboxylic acid.

5. Effect of Surface Treatments on Adsorption

5-1. Water Vapor Adsorption

The role and involvement of surface functional groups in the adsorption process were examined by studying the equilibrium adsorption in both vapor phase (water vapor) and liquid phase (metal ions). In water adsorption, it has been stated that the role of acidic groups is to act as a primary active site for water molecules to first adsorb on, followed by self adsorption among water molecules via hydrogen bonding, leading to the growing of water cluster as the pres-

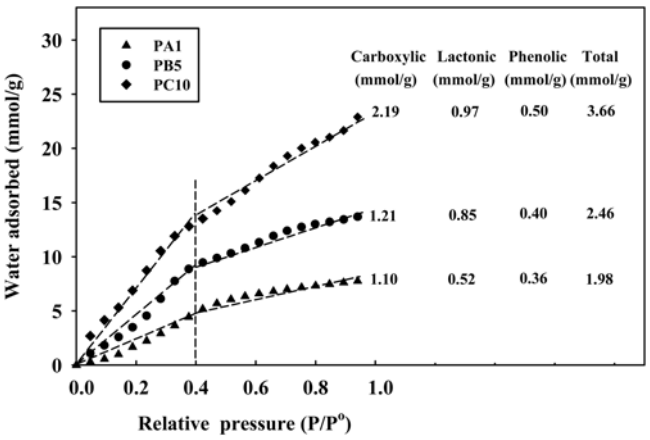

Fig. 6. Water adsorption isotherms at 30 °C of fully oxidized activated carbons with nitric acid.

sure is increased [22-24,41-42]. Fig. 6 shows water isotherms at 30 °C of three oxidized carbons that contained the maximum content of introduced acidic surface groups (PA1, PB5 and PC10). As a result, the adsorption behavior of these carbons would depend chiefly on the role of functional groups with relatively less effect of physical adsorption by dispersive forces on hydrophobic graphene layers. As observed, the isotherm curves shifted systematically upward with increasing content of total acidic groups, indicating that the increased water adsorption is due principally to the contribution of acidic surface groups. Further examination of Fig. 6 shows that the isotherm curves can be approximated by two straight lines intersecting at P/P^o~0.4. The slope of this straight line, which can be viewed as the differential increasing of adsorbed amount with respect to the change in relative pressure, is higher for adsorption at P/P^o< 0.4. Therefore, the faster response of the amount adsorbed with increasing pressure suggests that the acidic groups could concentrate more in the smaller pores corresponding to adsorption in the pressure range P/P^o<0.4, as compared to the adsorption in the larger pores at higher relative pressures. To test this proposed hypothesis of acidic group concentration in small pore sizes without resorting to sophisticated analytical procedures, the Monte Carlo simulation technique [43-46] may be alternatively used to compute the distribution of acidic surface groups as a function of pore size based on the best fitting of simulated results and the experimentally measured isotherm data. The use of this simulation approach will be our next investigation task.

Fig. 7 compares the water isotherms of two fully oxidized carbons originally prepared by physical and chemical activation and having comparable internal surface areas. It is interesting that sample PC10, which contains lesser amount of total acidic groups but with higher amount of carboxylic acid, could adsorb more water as compared to the adsorption of CN5-24. This demonstrates the major role of carboxylic acid in water adsorption, presumably due to its presence in relatively high amount and having higher polarity in comparison with lactonic and phenolic groups.

Fig. 8 compares the water isotherms of three activated carbons containing the least amount (sample C), intermediate amount (sample CN1-24) and maximum amount (sample CN5-24) of acidic surface groups. It is observed that the adsorption behavior can be divided into two regions for the relative pressures above and below 0.45, at which the isotherm curve of sample C starts to cross over. For adsorption at P/P^o<0.45, the amount of water adsorbed increased systematically with increasing content of acidic groups, indicating that water adsorption in this region is controlled predominantly by the effect of surface functional groups. The importance of the carbon surface groups for water adsorption in the region of low and medium relative pressures was also recognized by Rodriguez-Reinoso et al. [25]. However, for P/P^o>0.45, where adsorption occurs in the larger pores and at higher adsorbate concentration, the adsorption characteristics are somewhat complicated. The amount of water adsorbed was still highest for sample CN5-24, obviously due to its possession of a large number of acidic surface groups over the whole range of pore sizes. On the adsorption of the original car-

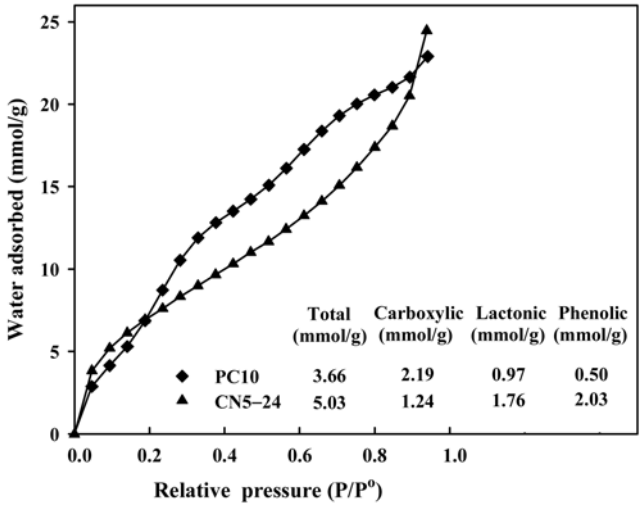

Fig. 7. Comparison of water adsorption isotherms at 30 °C of oxidized carbon having comparable surface area of the original carbons but with significant difference in acidic oxygen functional groups.

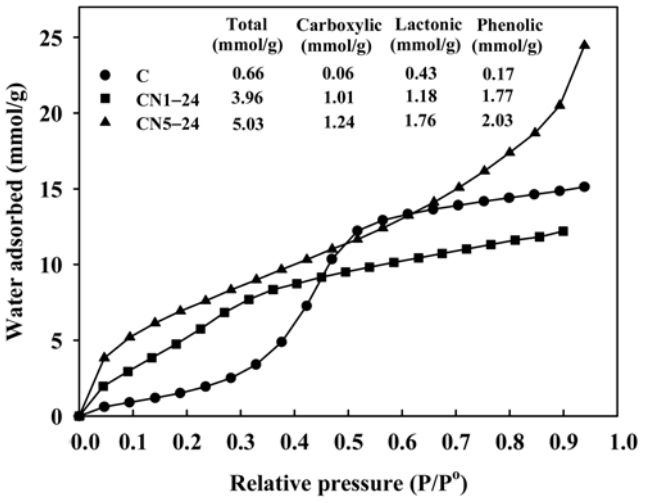

Fig. 8. Water adsorption isotherms at 30 °C of chemically activated carbon and activated carbons with two different degrees of oxidation with HNO_3.

bon, the adsorption capacity surpassed that of sample CN1-24 and stayed parallel to each other over the remaining range of relative pressure; this behavior may be explained as follows. Water adsorption of the original carbon, which contains almost no functional groups, involves the adsorption on hydrophobic carbon surface by weak adsorbent-adsorbate interaction forces. Adsorption by this mechanism is inefficient at a low pressure (low concentration) for a polar molecule like water. However, at a higher pressure, where adsorption occurs in larger pore sizes, the high density of adsorbate in the bulk gas phase can force water molecules to enter and pack inside the pores with the help of self hydrogen bonding and this would lead to a sharp increase of the adsorbed amount as the pressure is increased. On the other hand, adsorption of sample CN1-24 employs both functional groups and pore packing effects. However, the pore volume available for physical adsorption inside the pores for this carbon is much reduced caused by the partial blocking of pore entrance due to the presence of introduced surface groups at the edges of graphitic layers. The overall effect is to make the adsorption capacity of CN1-24 to be less than that of the original carbon.

Fig. 9 shows the equilibrium water isotherms of the oxidized carbons (PB1) before and after heat treatment at 600 °C (sample PB1-HT1) and 800 °C (sample PB1-HT2). It should be remembered that sample PB1 is not a fully oxidized carbon. Therefore, it is anticipated that water adsorption of this carbon should depend both on the role of functional groups and dispersive interaction on normal graphitic planes. The result indicates that the decrease in acidic group concentration due to heat treatment process resulted in the lowering of water adsorbed for adsorption at $P/P^o<0.6$. This decrease in

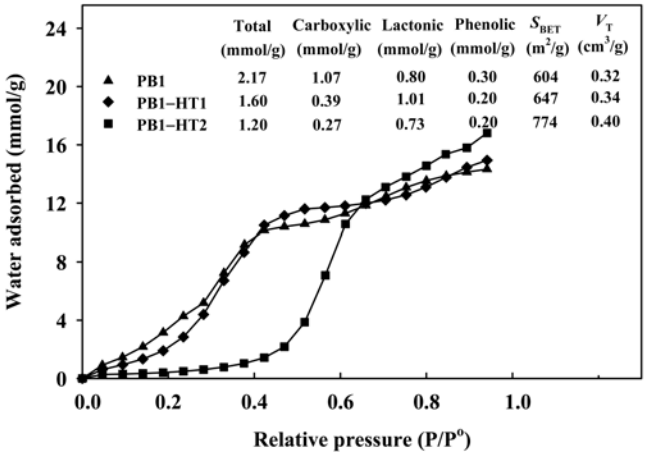

Fig. 9. Water adsorption isotherms at 30 °C of original, oxidized, and heat treated activated carbons.

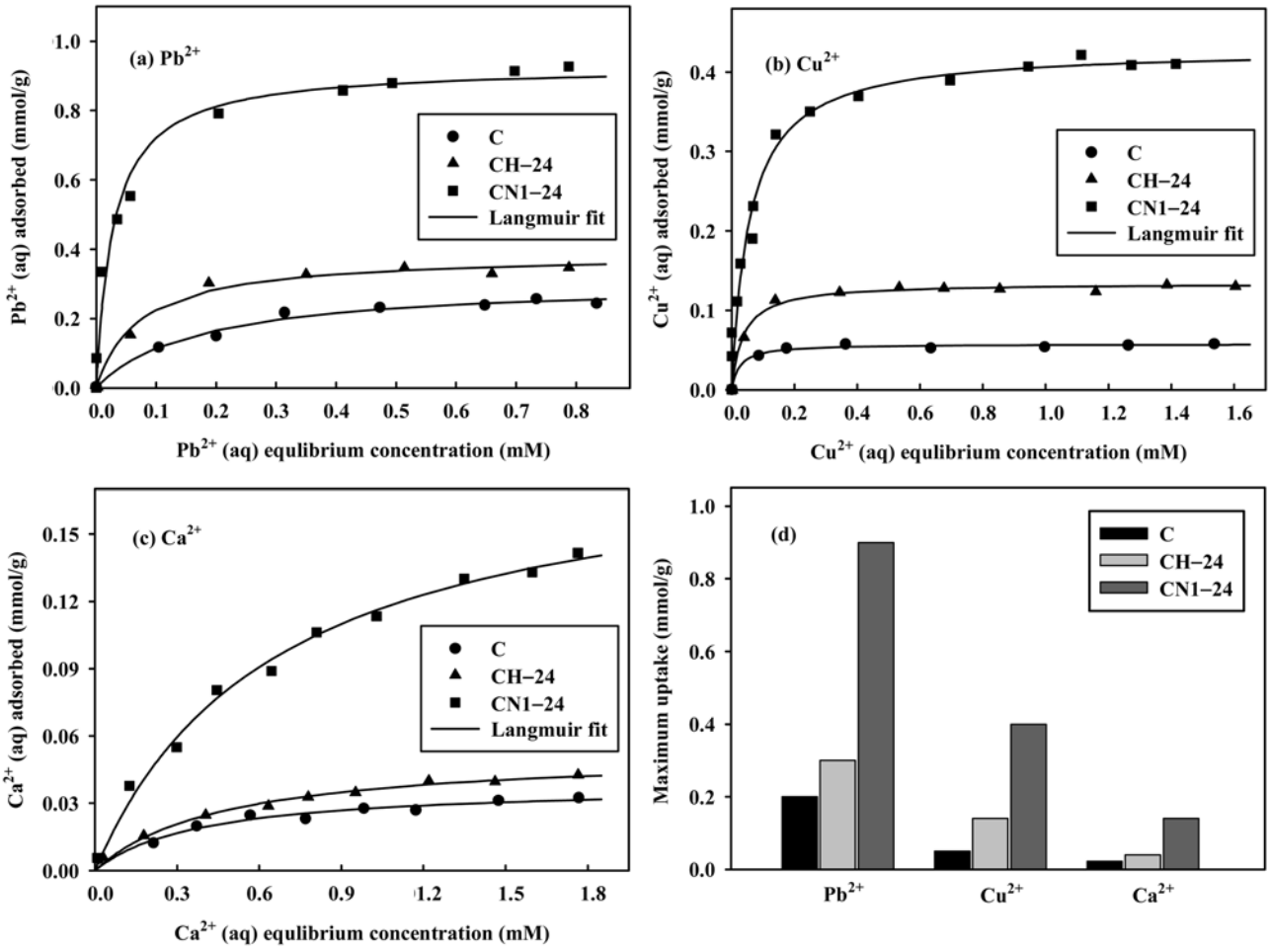

Fig. 10. Adsorption isotherms of (a) Pb^{2+}, (b) Cu^{2+} and (c) Ca^{2+} on original and oxidized activated carbons at 30 °C and (d) maximum uptake of metal ions on each carbon sample.

the amount adsorbed is also accompanied by the reduction of carboxylic acid content, although not proportionally. For $P/P^o>0.6$, adsorption on hydrophobic surfaces and pore packing in larger pore sizes came into play as previously discussed, with sample PB1-HT2 showing greater adsorption capacity largely because of its higher surface area and pore volume. Again, by noticing the shape of isotherm curves as in the case of Fig. 6, it is postulated that surface functional groups of PB1 and PB1-HT1 might concentrate more in small pores, corresponding to adsorption for $P/P^o<0.6$, so that adsorption at higher relative pressures would be determined to a greater extent by the porous structure of activated carbon.

5-2. Heavy Metal Adsorption

For liquid-phase adsorption, Figs. 10(a)-(c) show, respectively, the equilibrium isotherms of Pb^{2+}, Cu^{2+} and Ca^{2+} adsorbed on the original and two oxidized carbons having different degree of oxidation. All isotherms can be well described by the Langmuir adsorption model,

$$q_e=q_m\, b\, C_e/(1+bC_e),$$

where q_e is the adsorbed amount of metal ion at equilibrium, q_m is the maximum amount adsorbed, b is the affinity coefficient and C_e the equilibrium concentration in solution. It is seen that the surface oxidized carbons could enhance the adsorption level of all metal ions, as compared to that of the original carbons. Based on the maximum uptake (q_m), Fig. 10(d) shows that sample CN1-24 gave the highest increase of 200% , 600% and 380% for adsorbing Pb^{2+}, Cu^{2+} and Ca^{2+}, respectively, as compared to adsorption with the original carbon. For sample CH-24, which contains lesser amounts of acidic surface groups, the percentage increase of Pb^{2+}, Cu^{2+} and Ca^{2+} was about 30%, 120% and 25%, respectively. The much higher uptake of Pb^{2+} than that of Cu^{2+} and Ca^{2+} was ascribed to the higher electronegativity of Pb^{2+} (2.33 for Pb^{2+}>1.90 for Cu^{2+}>1.00 for Ca^{2+}), thus enabling higher affinity for adsorption sites on the carbon surfaces [47]. As Fig. 11 shows, there exists a linear correlation between acidic group concentration and the maximum uptake, thus demonstrating the key role of acidic surface groups in metal ion adsorption.

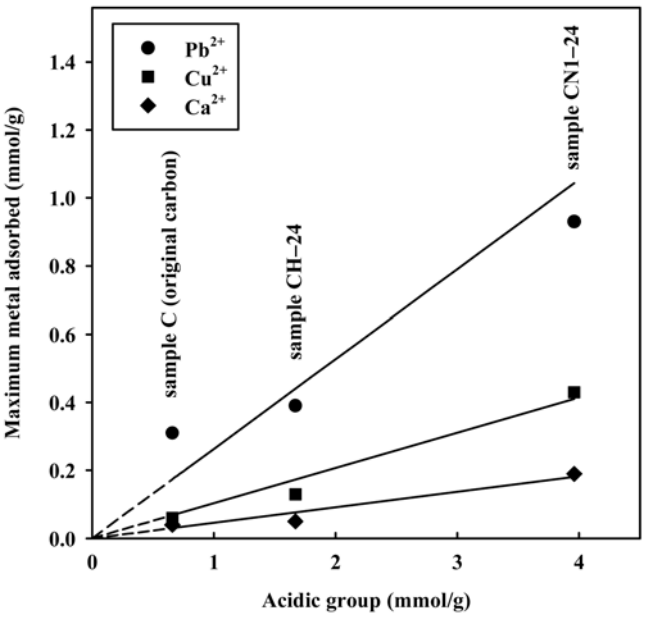

Fig. 11. Relationship between maximum amounts of metal ions adsorbed (q_m) and content of acidic functional groups.

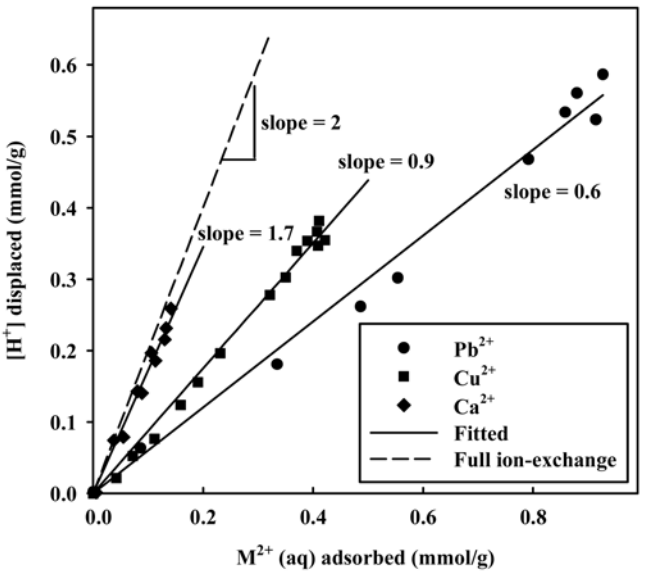

Fig. 12. Relationship between proton exchange capacity and metal ion uptake for sample CN1-24.

A number of investigations [6,14,18,21] have shown that the adsorption of metal ions on an oxidized carbon occurs generally by the exchange of metal ion with protons released from acidic surface groups. Therefore, the solution pH was measured in the present study before and after the adsorption tests. A decrease in the pH was observed, for example, the solution pH after the adsorption of Pb^{2+} was found to vary in the range 2.92-3.88 compared to the value of 5.5 for the initial feed solution, and thus confirming that the metal ions did displace protons from the acidic surface groups by ion-exchange process. Fig. 12 shows a linear relationship between the adsorbed amounts of all metal ions and the amount of proton displacement for sample CN1-24. It can be seen that the curve of Ca^{2+} (slope 1.7) is closest to the line of true-ion exchange (slope=2), coinciding with the stoichiometry of cation exchange. That is, two hydrogen ions are released from the oxidized carbon to the solution by each mole of metal ion adsorbed and thus involving mainly with carboxylic acid which has the highest ion-exchange capacity:

$$2(\text{-COOH})+M^{2+} \quad (\text{-COO})_2M^{2+}+2H^+$$

It is noteworthy that for the adsorption of transition metal ions (Cu^{2+} and Pb^{2+}), both curves lie well below the line of true ion-exchange (slope=0.9 and 0.6, respectively), indicating less contribution from cation exchange to the adsorption of these ions. This appears to indicate that the adsorption of Pb^{2+} and Cu^{2+} under the conditions studied not only involves the ion-exchange mechanism but also the other mechanism that could involve the interaction between the metal ions and other different types of acidic surface groups. Thus, the various forms of surface functional groups other than carboxylic acid that can participate more in the adsorption are the main reason for the much higher uptake of Cu^{2+} and Pb^{2+} than that of Ca^{2+}. Both roles of ion-exchange and other complex formation were also previously observed and proposed for the adsorption of Pb^{2+}, Cu^{2+} and

other heavy metal ions such as Cr^{3+}, Cd^{+2}, Co^{+2} and Zn^{+2} [9,17,48].

CONCLUSIONS

Fixation of oxygen functional groups onto the surface of eucalyptus wood-based activated carbons with the purpose of increasing their hydrophilic character was carried out by oxidative liquid treatment with H_2O_2, $(NH_4)_2S_2O_8$ and HNO_3, and gas treatment with air under varying degree of oxidation. It was found that the increasing level of oxidation treatment gave rise to a corresponding increase in the number of acidic surface groups and a decrease in basic site content (except with nitric acid oxidation). After oxidation, the carboxylic acid group showed the largest percentage increase in its content followed by phenolic and lactonic groups, whereas the order of acidic group distribution remained unaffected. Of all the oxidants used and under the treatment conditions studied, air oxidation at the highest permissible temperature of 350 ºC was effective in producing the highest content of total acidic surface group as well as carboxylic acid. For this study in which eucalyptus wood was used as a precursor, the activation temperature and/or oxidizing temperature may be used to manipulate the creation and distribution of various acidic surface groups in the oxidized carbon. It is desirable to employ physically activated carbon for surface oxidation if high carboxylic acid content is a prerequisite, whereas chemically activated carbon is the primary choice to obtain the largest creation of total acidic and lactonic groups. Another important finding from this work is the demonstration that a given activated carbon can be fully oxidized to obtain a maximum acidic group content using a certain minimum nitric acid concentration that increases proportionally with increased surface area and porosity of the carbon.

To achieve maximum adsorption of a polar adsorbate (water vapor) or metal ion species, it is best to use an oxidized carbon that contains the largest content of oxygen functional groups, with carboxylic acid contributing most in the adsorption process. The adsorption capacity of water by a surface oxidized carbon is determined both by the role of oxygen surface groups and dispersive interaction on the grapheme layer surfaces, with the latter mechanism starting to gain its importance when the relative pressure of water adsorption exceeds the value of about 0.5. The adsorption of a metal ion from solution relies on its ion exchange with proton-releasing surface groups as well as surface complex formation with all forms of surface functionalities. The relative contribution of these two mechanisms depends on the nature of metal ion and the proportion of various existing acidic groups on the carbon surface.

ACKNOWLEDGMENTS

The authors would like to thank Suranaree University of Technology for financial support of this work under SUT Research Funds (Contract No. 3/2551).

REFERENCES

1. R. C. Bansal and M. Goyal, *Activated carbon adsorption*, CRC Press, Florida (2005).
2. M. V. Lopez-Ramon, F. Stoeckli, C. Moreno-Castilla and F. Carrasco-Marin, *Carbon*, **37**, 1215 (1999).
3. J. A. Menendez, J. Phillipse, B. Xia and L. R. Radovic, *Langmuir*, **12**, 4404 (1996).
4. S. S. Barton, M. J. B. Evans, E. Halliop and J. A. F. MacDonald, *Carbon*, **35**, 1361 (1997).
5. L. R. Radovic, I. F. Silva, J. I. Ume, J. A. Menendez, C. A. Leon y Leon and A. W. Scaroni, *Carbon*, **35**, 1339 (1997).
6. Y. F. Jia and K. M. Thomas, *Langmuir*, **16**, 1114 (2000).
7. C. Moreno-Castilla, M. V. Lopez-Ramon and F. Carrasco-Marin, *Carbon*, **38**, 1995 (2000).
8. M. A. Montes-Moran, D. Suarez, J. A. Menendez and E. Fuente, *Carbon*, **42**, 1219 (2004).
9. J. Jaramillo, V. Gomez-Serrano and P. M. Alvarez, *J. Hazard. Mater.*, DOI:10.1016/j.jhazmat.2008.04.009 (2008).
10. P. Vinke, M. Eijk, M. Verbree and A. F. Voskamp, *Carbon*, **32**, 675 (1994).
11. J. Choma, W. Burakiewicz-Mortka, M. Jaroniec, Z. Li and J. Klinik, *J. Colloid Interface Sci.*, **214**, 438 (1999).
12. J. L. Figueiredo, M. F. R. Pereira, M. M. A. Freitas and J. J. M. Orfao, *Carbon*, **37**, 1379 (1999).
13. M. Domingo-Garcia, F. J. Lopez-Garzon and M. Perez-Mendoza, *J. Colloid Interface Sci.*, **222**, 233 (2000).
14. M. Goyal, V. K. Rattan, D. Aggarwal and R. C. Bansal, *Colloids Surf. A*, **190**, 229, (2001).
15. G. S. Szymanski, Z. Karpinski, S. Biniak and A. Swiatkowski, *Carbon*, **40**, 2627 (2002).
16. D. Aggrarwal, M. Goyal and R. C. Bansal, *Carbon*, **37**, 1989 (1999).
17. V. Jr. Strelko and D. J. Malik, *J. Colloid Interface Sci.*, **250**, 213 (2002).
18. A. Swiatkowski, M. Pakula, S. Biniak and M. Walczyk, *Carbon*, **42**, 3057 (2004).
19. B. Xiao and K. M. Thomas, *Langmuir*, **20**, 4566 (2004).
20. S. Haydar, M. A. Ferro-Garcia, J. Rivera-Utrilla and J. P. Joly, *Carbon*, **41**, 387 (2003).
21. S. Sato, K. Yoshida, K. Moriyama, M. Machida and H. Tatsumoto, *Appl. Surf. Sci.*, **253**, 8554 (2007).
22. M. M. Dubinin and M. M. Serpinsky, *Carbon*, **19**, 402 (1981).
23. K. Kaneko, Y. Hanazawa, T. Iiyama, T. Kanda and T. Suzuki, *Adsorption*, **5**, 7 (1999).
24. D. D. Do and H. D. Do, *Carbon*, **38**, 767 (2000).
25. F. Rodriguez-Reinoso, M. Molina-Sabio and M. A. Munecas, *J. Phys. Chem.*, **96**, 2707 (1992).
26. C. Moreno-Castilla, M. A. Ferro-Garcia, J. P. Joly, I. Bautista-Toledo, F. Carrasco-Marin and J. Rivera-Utrilla, *Langmuir*, **11**, 4386 (1995).
27. V. Jr. Strelko, D. J. Malik and M. Streat, *Carbon*, **40**, 95 (2002).
28. A. H. El-Sheikh, *Talanta*, **75**, 127 (2008).
29. Y. Ngernyen, C. Tangsathitkulchai and M. Tangsathitkulchai, *Korean J. Chem. Eng.*, **23**, 1046 (2006).
30. A. Klijanienko, E. Lorence-Grabowska and G. Gryglewicz, *Bioresour. Technol.*, **99**, 7208 (2008).
31. P. Patnukao and P. Pavasant, *Bioresour. Technol.*, **99**, 8540 (2008).
32. D. D. Do, *Adsorption analysis: Equilibria and kinetics*, Imperial College Press, Singapore (1998).
33. H. P. Boehm, *Adv. Catal.*, **16**, 179 (1966).
34. H. P. Boehm, *Carbon*, **32**, 759 (1994).
35. F. Rouquerol, J. Rouquerol and K. Sing, *Adsorption by powders and porous solids*, Academic Press, London (1999).
36. C. Moreno-Castella, F. Carrasco-Marin, F. J. Maldonado-Hodar and

J. Rivera-Utrilla, *Carbon*, **36**, 145 (1998).
37. G. de la Puente, J. J. Pis, J. A. Menendez and P. Grange, *J. Anal. Appl. Pyrolysis*, **43**, 125 (1997).
38. M. Domingo-Garcia, F. J. Lopez-Garzon and F. J. Perez-Mendoza, *J. Colloid Interface Sci.*, **248**, 116 (2002).
39. A. Contescu, M. Vass, C. Contescu, K. Putyera and J. A. Schwarz, *Carbon*, **36**, 247 (1998).
40. T. Cordero, J. Rodriguez-Mirasol, N. Tancredi, J. Piriz, G. Vivo and J. J. Rodriguez, *Ind. Eng. Chem. Res.*, **41**, 6042 (2002).
41. G. R. Birkett and D. D. Do, *Mol. Phys.*, **104**, 623 (2006).
42. S. Junpirom, C. Tangsathitkulchai, M. Tangsathitkulchai and Y. Ngernyen, *Korean J. Chem. Eng.*, **25**, 825 (2008).
43. M. P. Allen and D. J. Tildesley, *Computer simulation of liquids*, Clarendon Press, Oxford (1987).
44. D. Frenkel and B. Smit, *Understanding molecular simulation: From algorithms to application*, Academic Press, San Diego (2001).
45. W. A. Steele, *Appl. Surf. Sci.*, **196**, 3 (2002).
46. D. D. Do and H. D. Do., *Adsorpt. Sci. Technol.*, **21**, 389 (2003).
47. S. A. Dastgheib and D. A. Rockstraw, *Carbon*, **40**, 1843 (2002).
48. M. Pesavento, A. Profumo, G. Alberti and F. Conti, *Anal. Chim. Acta*, **480**, 171 (2003).